

## A COMPARISON OF SCATTERING CROSS-SECTIONS OF SPHERICAL PARTICLES AND BUBBLES

by

A. J. PATITSAS

(Department of Physics, Fine Particle Research Institute, Laurentian University  
Sudbury, Ontario, Canada)

(Received 5-4-78)

**Abstract:** *The forward and back scattering cross-sections of a spherical particle of radius  $a$  and of complex refractive index  $N_1$  lying in a medium of real refractive index  $N_2$ , and the same scattering cross-sections of a spherical bubble of radius  $a$  and of real refractive index  $N_2$  lying in a slightly conducting medium of complex refractive index  $N_1$  ( $|N_1| > N_2$ ), are determined and compared in the Rayleigh domain where  $\alpha = 2\pi a/\lambda \leq 0.3$  and also are computed and compared in the Mie domain,  $0.3 < \alpha \leq 22.0$ . The real part of the refractive index  $N = N_1/N_2$  is assigned the values 1.1, 1.3, 1.5 and 2.1 while the imaginary part of  $N$  is changed in small steps from 0.01 to 0.11. The ratios of the scattering cross-sections of the particle to those of the bubble are presented in graphical form. The scalar theory is also utilized in computing the scattering cross-sections of particles and bubbles and the results are compared in graphical form with those utilizing the Mie theory.*

### INTRODUCTION

A spherical particle of radius  $a$  and complex refractive index  $N_1 = N_{1r} + iN_{1i}$  is assumed to lie in an infinite medium of real refractive index  $N_2$ . A Cartesian coordinate system is introduced with its origin coinciding with the center of the particle. A plane electromagnetic wave linearly polarised with its  $E$  vector along the  $x$ -axis and having wavelength  $\lambda_2$  is assumed to be incident on the particle from the  $-z$  direction toward the  $+z$  direction. It is assumed that  $\lambda_2 \gg a$  so as the scattering lies in the Rayleigh domain. From Stratton<sup>7</sup>, page 436, it can be seen that the time average power scattered by the particle in the forward hemisphere,  $0^\circ \leq \theta \leq 90^\circ$ ,  $\theta$  being the polar angle measured from the  $+z$  axis, or equally in the backward hemisphere,  $90^\circ \leq \theta \leq 180^\circ$ , is given by the expression

$$W^{(p)} = N_{2r} \frac{k_0^3 \omega}{\varepsilon_0} \frac{1}{24\pi} |p^{(1)}|^2 \quad (1)$$

where  $k_0 = 2\pi/\lambda_0$  = wave number in vacuum,  $\varepsilon_0$  = permittivity of free space,  $\omega$  = angular frequency of the incident wave, and  $p^{(1)}$  is the induced dipole moment in the particle. From Stratton<sup>7</sup>, page 572, it can be seen that

$$|p^{(1)}|^2 = 16\pi^2 a^6 |\varepsilon_2|^2 \left| \frac{N^2 - 1}{N^2 + 2} \right|^2 |E_0|^2 \quad (2)$$

where  $\varepsilon_2$  = the real permittivity of the medium,  $N = \frac{N_1}{N_2}$ , and  $E_0$  is the amplitude of the incident plane wave. Now  $\varepsilon_2 = N_2^2 \varepsilon_0$ , so when eq. (2) is used in eq. (1)  $W^{(p)}$  becomes,

$$W^{(p)} = \frac{2\pi}{3} k_0^3 \varepsilon_0 \omega a^6 |E_0|^2 N_{2r} |N_2|^4 \left| \frac{N^2 - 1}{N^2 + 2} \right|^2 \quad (3)$$

Now the roles of the refractive indices  $N_1, N_2$  are assumed reversed, i.e. a spherical particle (from now on termed bubble) of radius  $a$  and real refractive index  $N_2$  is assumed to lie in an infinite medium of complex refractive index  $N_1$ . The time average power scattered by the bubble in the forward or backward hemispheres may be obtained from eq. (3) by exchanging  $N_1, N_2$ , i.e.,

$$W^{(b)} = \frac{2\pi}{3} k_0^3 \varepsilon_0 \omega a^6 |E_0|^2 \frac{N_{1r}}{4} |N_1|^4 \left| \frac{N^2 - 1}{N^2 + \frac{1}{2}} \right|^2 \quad (4)$$

It should be anticipated here that in practice the medium would not be infinite but rather a film whose thickness is large compared with the radius of the bubble (particle) and whose complex refractive index  $N_1$  has an imaginary part sufficiently small so as the wave is little attenuated in traversing the film.

At this stage the ratio of  $W^{(b)}$  over  $W^{(p)}$  is considered. It is easy to show that

$$\frac{W^{(b)}}{W^{(p)}} = \frac{1}{4} \left( \frac{N_{1r}}{N_{2r}} \right) |N|^4 \left| \frac{N^2 + 2}{N^2 + \frac{1}{2}} \right|^2 \quad (5)$$

where as before  $N = \frac{N_1}{N_2}$

It can be seen that if  $|N| > 1$  or  $\frac{N_{1r}}{N_{2r}} > 1$ , since  $N_{1r} \gg N_{1i}$  and  $N_{2i} = 0$ ,

then  $\frac{W^{(b)}}{W^{(p)}} > 1$ ; i.e. in the Rayleigh domain a bubble has a larger cross-section than a particle of the same radius with the refractive indices of the media interchanged as described above. Thus for  $N = N_{1r}/N_{2r} = 1.5$ ,  $W^{(b)}/W^{(p)}$  equals 4.5343. It may be remarked here that the ratio in eq. (5) remains the same regardless of the state of the polarization of the incident plane wave. The state of polarization affects only the factor  $|E_0|^2$  in eq. (2) and this factor is assumed to be the same in both cases of particle scattering and bubble scattering, Stone<sup>6</sup> p. 101. It may be stated further that the ratio in eq. (5) is valid for a completely unpolarised incident beam.

The main objective of this work is the examination of the ratio in eq. (5) in the Mie domain where  $6\pi a \gg \lambda$ . The method of computation of the perpendicular and parallel Mie intensities  $i_1$ ,  $i_2$  is similar to that used by Denman et al,<sup>2</sup> i.e.,

$$i_1 = \frac{1}{2} \left( \frac{E_0^2}{\omega \mu} \right) \frac{1}{kr^2} \left| \sum_{n=1}^{\infty} (A_n \tau_n + B_n \pi_n) \right|^2 \quad (6)$$

$$i_2 = \frac{1}{2} \left( \frac{E_0^2}{\omega \mu} \right) \frac{1}{kr^2} \left| \sum_{n=1}^{\infty} (A_n \pi_n + B_n \tau_n) \right|^2 \quad (7)$$

where  $r$  is the distance from the center of the scattering sphere to the point in the far zone where  $i_1$ ,  $i_2$  are to be computed. In the present case  $r$  cancels out upon integrating  $i_1$ , and  $i_2$  over the forward and backward hemispheres. The expressions for the coefficients  $A_n$ ,  $B_n$ ,  $\tau_n$ ,  $\pi_n$  may be

found in an earlier publication, Patitsas<sup>3</sup>. Several typographical errors are to be noted there, i.e. the expressions for  $A_n$ ,  $B_n$  in eqs. (3a), (3b) are to be exchanged, the factor  $1/\alpha$  in the expression for  $V_2$  should be replaced by  $n/\alpha$  and the expression for  $\pi_n$  should be as follows;

$$\pi_n = \frac{n}{x^2 - 1} (xP_n(x) - P_{n-1}(x))$$

When the medium in which the particle (bubble) lies is nonconducting,  $k$  is real and thus the expressions for  $i_1, i_2$  are real. But when the medium is conducting as is presently the case for the bubbles,  $k=k_1=k_0$ ,  $N_1=k_0(N_{1r}+iN_{1i})$ , i.e.  $k$  is complex. In this case  $i_1, i_2$  are equal to the real parts of the expressions in eqs. (6), (7); i.e. the factor  $1/k$  in these expressions should be replaced by

$$R_e \left( \frac{1}{k_0 N_1} \right) = R_e \left( \frac{1}{k_0} \frac{N_{1r} - i N_{1i}}{|N_1|^2} \right) = \frac{1}{k_0} \frac{N_{1r}}{|N_1|^2} \quad (8)$$

In the case of the particle in the non-conducting medium, the equivalent expression is

$$R_e \left( \frac{1}{k_0 N_2} \right) = \frac{N_{2r}}{k_0 |N_2|^2} = \frac{1}{k_0 N_2} \quad (9)$$

since  $N_{2i}=0$ .

For a completely unpolarized incident beam the Mie scattering intensity is, Rosche<sup>5</sup>, Patitsas<sup>4</sup>,

$$i_e = \frac{i_1 + i_2}{2} \quad (10)$$

The integrals of  $i_e$  over the forward and backward hemispheres are now termed  $I_r^{(p)}$ ,  $I_b^{(p)}$  respectively for the case of the particle causing the scattering, and  $I_r^{(b)}$ ,  $I_b^{(b)}$  for the case of the bubble causing the scattering. In the Rayleigh domain the following relations ought to hold

$$\frac{I_r^{(b)}}{I_r^{(p)}} = \frac{I_b^{(b)}}{I_b^{(p)}} = \frac{W^{(b)}}{W^{(p)}} \quad (11)$$

Thus, if the products  $R_r$ ,  $R_b$  are formed as follows,

$$R_r = \frac{I_r^{(p)}}{I_r^{(b)}} = \frac{W^{(b)}}{W^{(p)}} \quad (12)$$

$$R_b = \frac{I_b^{(p)}}{I_b^{(b)}} = \frac{W^{(b)}}{W^{(p)}} \quad (13)$$

then  $R_r \approx R_b \approx 1$  in the Rayleigh domain. The behavior of  $R_r$ ,  $R_b$  as functions of the size parameter  $\alpha = 2\pi a/\lambda$  from the Rayleigh region,  $\alpha \leq 0.3$ , to well into the Mie region is presented in the following section. The integration of  $i_e$  over the forward (backward) hemisphere involves the integration over the azimuthal angle  $\varphi$ , which is easily done since  $\varphi$  enters only as  $\sin^2 \varphi$  and  $\cos^2 \varphi$ , Patitsas<sup>4</sup>, and the integration over the polar angle  $\theta$ , which was done numerically by computing  $i_1$ ,  $i_2$  for a given  $\alpha$ ,  $N$  in steps of  $\Delta\theta = 0.5^\circ$ . This angular step is sufficiently small so as not to cause any appreciable error in replacing the integral over  $\theta$  by a finite sum. It may be noted that the angular distance between the first minimum and the first maximum of  $i_1$  for  $\alpha = 4.0$ ,  $N = 1.333$  is approximately  $20^\circ$ , Denman et al<sup>2</sup>.

The scattering intensities  $i_1$ ,  $i_2$  were computed with an accuracy of four significant figures. For several arbitrary values of  $\alpha$ ,  $N$  and  $\theta$ ,  $i_1$ ,  $i_2$  were also computed using the Mie subroutines by Dave<sup>1</sup>. In all cases the two methods of computation gave the same values for  $i_1$ ,  $i_2$  up to four significant figures. The scalar scattering intensity  $i_s$  may be written as, Patitsas<sup>3</sup>,

$$i_s = \frac{1}{2} \left( \frac{E_\theta^2}{\omega \mu} \right) \frac{1}{kr^2} \left| \sum_{n=0}^{\infty} n(n+1) A_n P_n \right|^2 \quad (14)$$

where  $P_n$  is the Legendre polynomial and  $A_n$  is the same as in eqs. (6), (7). In the Rayleigh limit,  $\alpha \rightarrow 0$ , only the first term in the expansions (6), (7) and (14) may be kept. It can easily be shown that in this limit the ratio of the integral of  $i_e$  over the forward or backward hemisphere to that of  $i_s$  is,

$$I_e/I_s = Q = \frac{6}{(n^2+2)^2} \quad (15)$$

In the following section the variation of  $Q$  with  $\alpha$  will be presented for  $0.20 \leq \alpha \leq 9.00$  for various values of  $N$ .

### RESULTS

In Figure 1 the logarithm to the base ten of  $R_r$  is plotted versus the logarithm to the base ten of the size parameter  $\alpha$  for real values of  $N=N_1/N_2$  equal to 1.1, 1.3, 1.5 and 2.1. For the preparation of this plot the parameter  $\alpha$  was changed in steps of 0.20 from  $\alpha \sim 0.20$  to  $\alpha \sim 4.00$  and in steps of 1.00 from  $\alpha=4.00$  to  $\alpha=22.00$ . For these values of  $N$ , the values of  $W^{(b)}/W^{(p)}$  given by eq. (5) are respectively 1.4187, 2.6352, 4.5343 and 17.4016. Firstly it is observed that  $\log R_r \rightarrow 0.0$  i.e.  $R_r \rightarrow 1$  as  $\log \alpha \rightarrow -0.600$ , i.e. as  $\alpha \rightarrow 0.25$  for all  $N$  in agreement with the Rayleigh theory. As  $\alpha$  increases toward the Mie domain,  $R_r$  increases in all four cases of different  $N$ . For the case of  $N=1.1$ ,  $R_r$  increases to 1.4925 at  $\log \alpha=0.4624$ , or at  $\alpha=2.90$ . From eq. (12) it can be seen that

$$\frac{I_r^{(p)}}{I_r^{(b)}} = R_r \frac{W^{(p)}}{W^{(b)}} = 1.4925/1.4187 = 1.0520 \quad (16)$$

Thus, in the case of  $N=1.1$  the forward scattering cross - section of the particle divided by that of the bubble increases from  $1/1.4187$  at  $\alpha=0.25$  to 1.0520 at  $\alpha=2.90$  and then it stays practically at this value up to  $\alpha=22.00$ . In the case of  $N=1.3$ ,  $R_r$  rises to 2.9427 at  $\alpha=2.90$  and thus, at this value of  $\alpha$  eq. (16) becomes

$$\frac{I_r^{(p)}}{I_r^{(b)}} = 2.9427/2.6352 = 1.1167$$

There is a dip at  $\log \alpha=1.192$  or  $\alpha=15.56$ . In the case of  $N=1.5$  and  $N=2.1$ ,  $R_r$  peaks at approximately the same value of  $\alpha=2.90$  as for  $N=1.1$  and  $N=1.3$ . The values of  $I_r^{(p)}/I_r^{(b)}$  at  $\alpha=2.90$  are respectively equal to 1.1852 and 1.3961. There is an appreciable dip in  $R_r$  for  $N=1.5$  at  $\log \alpha=1.0792$ , or  $\alpha=12.00$  where  $I_r^{(p)}/I_r^{(b)} = 0.5490$ , and there is an appreciable dip in  $R_r$  for  $N=2.1$  at  $\log \alpha=0.8451$  or  $\alpha=7.00$  where  $I_r^{(p)}/I_r^{(b)} = 0.2533$ .

In figure 2  $\log R_b$  is plotted versus  $\alpha$  for the same values of  $N$  as in Figure 1. These plots behave overall as those in Figure 1 except for an appreciable increase in the number of peaks and dips as is generally the case in Mie scattering in the backward direction, Patitsas<sup>3</sup>. At the pronounced peaks at  $\log \alpha$  equal to 0.4914, 0.5185, 0.6020, and 0.6990 for  $N=1.1, 1.3, 1.5$  and  $2.1$  respectively, the ratio  $I_b^{(p)}/I_b^{(b)}$  has the respective values, 2.5544, 5.5893, 6.1552, and 4.5630. At the corresponding pronounced dips at  $\log \alpha$  equal to 0.6021, 0.6021, 0.6990, and 0.9031, the ratio  $I_b^{(p)}/I_b^{(b)}$  has the corresponding values, 1.2588, 3.0422, 4.4585, and 1.6459. It can be stated that for values of  $\log \alpha > 0.3200$ , or  $\alpha > 2.09$  the back scattering cross - section for the particle is considerably larger than that for the bubble for all real  $N > 1.1$ .

In Figure 3  $\log R_r$  is plotted versus  $\alpha$  for the real part of  $N$ ,  $NR=1.1$  and for several imaginary parts  $NI$  of  $N$  ranging from 0.0 to 0.11 printed near each graph on the right hand side of the Figure. The graphs for all  $NI > 0.05$  may be extended toward the point where the graph for  $NI=0.06$  ends, i.e. for all  $NI$ ,  $R_r \rightarrow 1.0$  as  $\alpha \rightarrow 0.20$ . The same may be stated for all graphs which appear in the following Figures 4-10. The same plots are repeated in Figures 4 and 5 but for  $NR=1.30, 1.50$ , while in Fig. 6, for  $NR=2.10$ , the crowding of the graphs allowed only those plots for  $NI=0.00, 0.03, 0.06$ , and  $0.11$  to be presented. The implication of these plots is clear, i.e. the introduction of a small imaginary part in  $N_r$ , or equivalently, a small conductivity in the medium making up the particle, causes  $R_r$  to decrease monotonically as  $NI$  increases; in other words, it renders the bubble a more efficient scatterer in the forward hemisphere as compared with the particle in this respect. It is seen that the smaller the value of  $NR$  the more pronounced is the effect of  $NI$ . In Figures 7-10  $\log R_b$  is plotted versus  $\alpha$  for the same values of  $NR, NI$  as in Figures 3-6 for  $\log R_r$ . The implication of these plots is the same as those for  $R_r$ . It can be seen, especially in Figures 7 and 8, that the effect of  $NI$  in reducing the value of  $R_b$  is more pronounced than that in the case of  $R_r$ .

The ratio  $I_c/I_s=Q$ , defined as the ratio of the intergral of  $i_c$  over the forward or backward hemisphere to that of  $i_s$ , is plotted versus,  $\alpha, 0.2 \leq \alpha \leq 9.0$ , in Figures 11, 12, and 13 for  $N$  equal to 1.20, 1.50 and 2.10 respectively. The subscripts of  $Q$ , i.e.  $f$  and  $b$  stand for the forward and backward hemispheres respectively, while the superscripts  $p$  and  $h$  stand for particle and bubble respectively. From eq. (15)  $Q_f^{(p)}$ , which equals  $Q_b^{(p)}$ , equals 0.5070, 0.3322 and 1.1460 for  $N=1.20, 1.50$  and  $2.10$  res-

pectively, while  $Q_r^{(b)}$ , which equals  $Q_b^{(b)}$ , equals 0.8264, 1.0041 and 1.2101 for the same values of  $N$ . It is observed that the values of  $Q$  for  $\alpha=0.2$  calculated by using eqs. (6), (7) and (14) agree quite well with those obtained from eq. 15, valid in the limit  $\alpha \rightarrow 0$ . In all three cases of different  $N$ ,  $Q_r^{(p)}$  and  $Q_r^{(b)}$  acquire values near one as  $\alpha \rightarrow 9.0$ . It may be stated that the forward scattering cross - section for particles and bubbles, may be computed using the relatively simple scalar theory when  $\alpha$  is not very small, i.e. not smaller than 4.0 in the case  $N=2.10$ . Values of  $Q_b^{(b)}$  and of  $Q_b^{(p)}$  for  $N=1.50$  and  $N=1.20$  respectively were computed for  $9.0 \leq \alpha \leq 24.0$ ; they remained quite near their values at  $\alpha=9.0$ . The computations which resulted in these plots were repeated for the imaginary part of  $N$ ,  $NI=0.05$ . It was observed that the only effect of  $NI$  was to reduce the amplitude of the oscillations of the plots, especially so for  $\alpha > 4.0$ . Thus the value of  $Q_b^{(p)}$  at  $\alpha=7.4$  and for  $NR=2.10$  is reduced from 1.92 to 1.30 when  $NI$  is increased from 0.00 to 0.05.

### CONCLUSION

In this paper, a particle has been defined as a spherical particle of radius  $a$  and complex refractive index  $N_1=N_{1r}+N_{1i}$  lying in a medium of real refractive index  $N_2$ . A bubble has been defined as a spherical particle of radius  $a$  and of real refractive index  $N_2$  lying in a medium of complex refractive index  $N_1$ . It has been found that in the Rayleigh domain, where the size parameter  $\alpha=2\pi a/\lambda$  is less than approximately 0.3, and for  $|N_1| > N_2$ , the bubble scatters a plane electromagnetic wave of arbitrary state of polarization more strongly than the particle, the case being more so as  $N=N_1/N_2$  increases. As  $\alpha$  becomes larger than 0.3, i.e. as the scattering enters into the Mie domain, the ratio of the forward scattering cross - section for the particle to that for the bubble increases for all cases of different  $N$  considered. It reaches a maximum of approximately one for  $\alpha \sim 3.0$ . The ratio of the back scattering cross - section of the particle to that of the bubble also increases as  $\alpha$  increases into the Mie domain. It becomes approximately one for all  $N$  considered for  $\alpha=2.0$  and it peaks to the value six at  $\alpha=4.0$  for  $N=1.50$ . The introduction of a small imaginary part in  $N_1$  or  $N$ , i.e. the introduction of a slight conductivity in the medium surrounding the bubble, results in a decrease in the ratio considered in both the forward and backward hemispheres, this being more so in the backward hemisphere. It has been deter-



mined that the forward scattering cross - section for particles and bubbles may be computed using the simple scalar theory as opposed to using the Mie theory for values of  $\alpha > 4.0$ .

#### Acknowledgement

The author wishes to thank Mr. M. Shaarani for his assistance in the computations, and preparations of the graphs, and for his comments and suggestions in the writing of the manuscript. Thanks are also due to Mr, P. Legault for preparing the final drawings of the graphs.

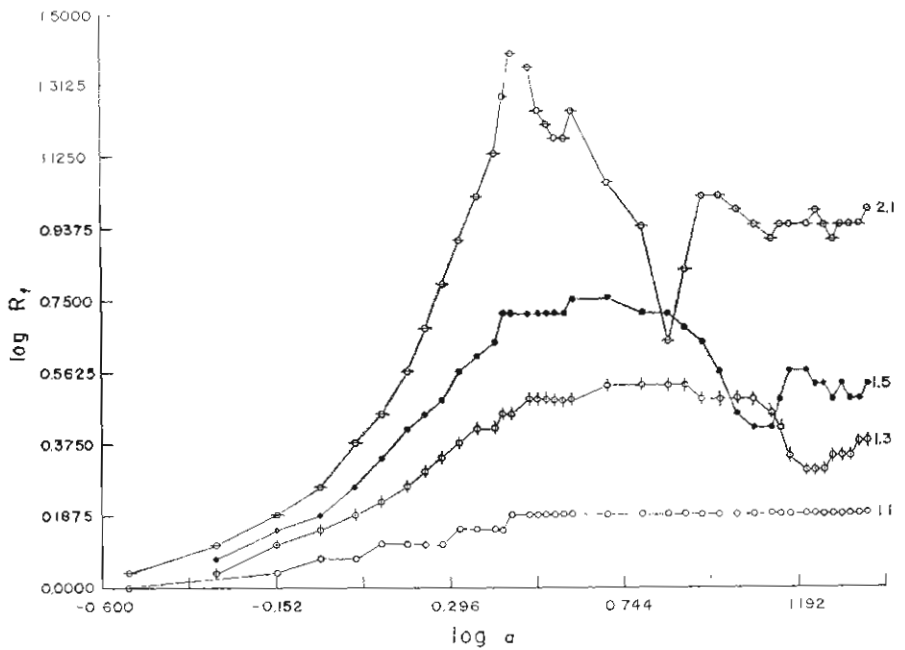


Figure 1 - The dependence on  $\alpha$  of the logarithm to the base ten of  $R_f$  = ratio of the forward scattering cross - section for particles to that for bubbles multiplied by the constant  $W^{(b)}/W^{(p)}$  for various real values of  $N$  shown at the right end of each graph.

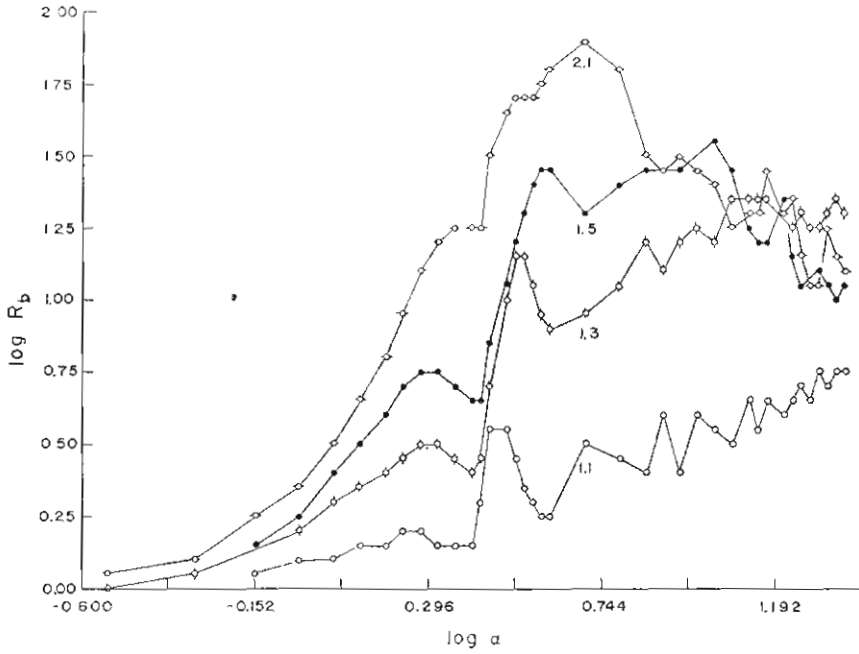


Figure 2 - Same as Figure 1 for Rb referring to the backward hemisphere.

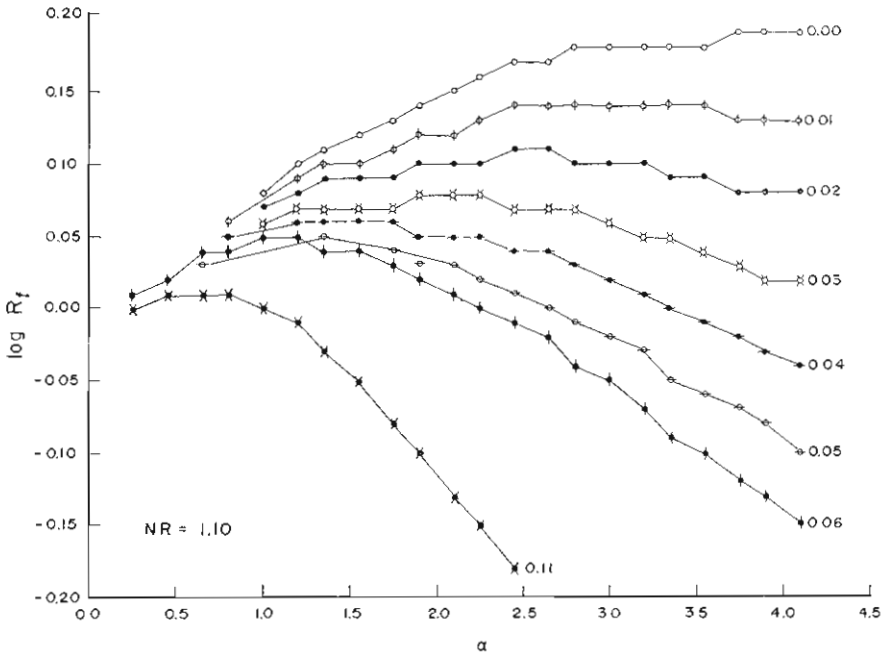


Figure 3 - Same as Figure 1 for real part of  $N$ ,  $NR=1.10$  and for various imaginary parts of  $N$ ,  $NI$  shown at the right end of each graph.

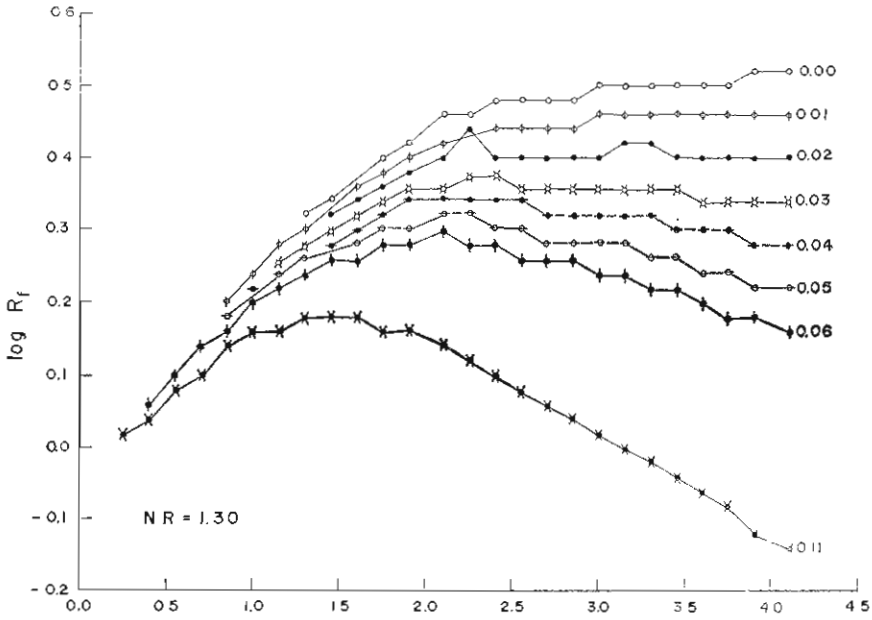


Figure 4 - Same as Figure 3 for  $NR=1.30$ .

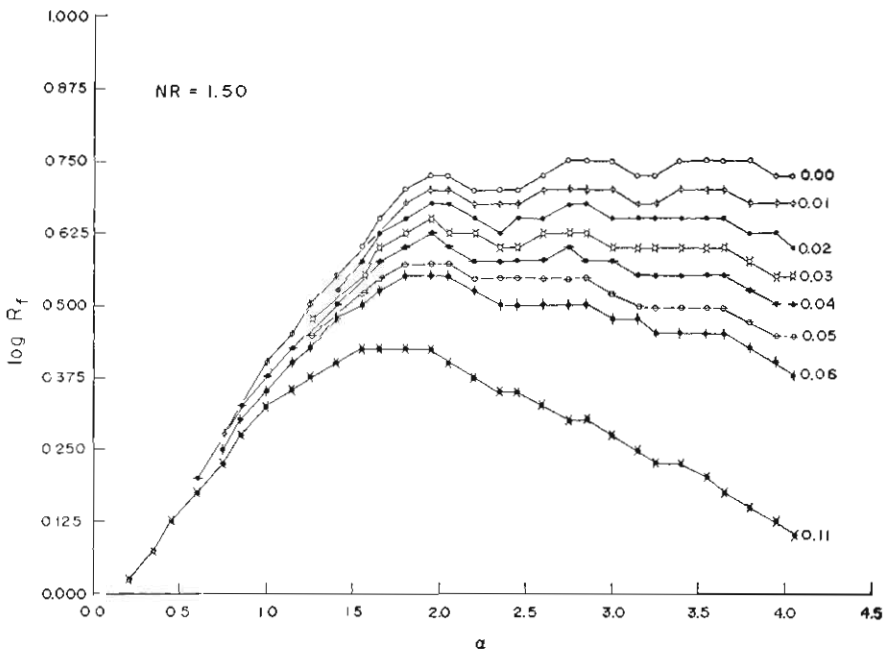


Figure 5 - Same as Figure 3 for  $NR=1.50$ .

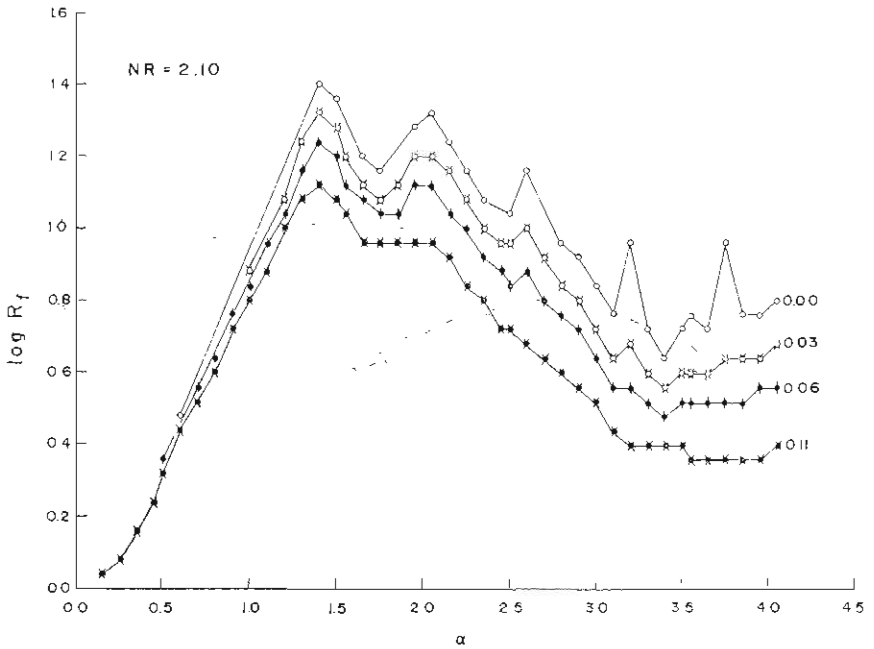


Figure 6 - Same as Figure 3 for  $NR=2.10$ .

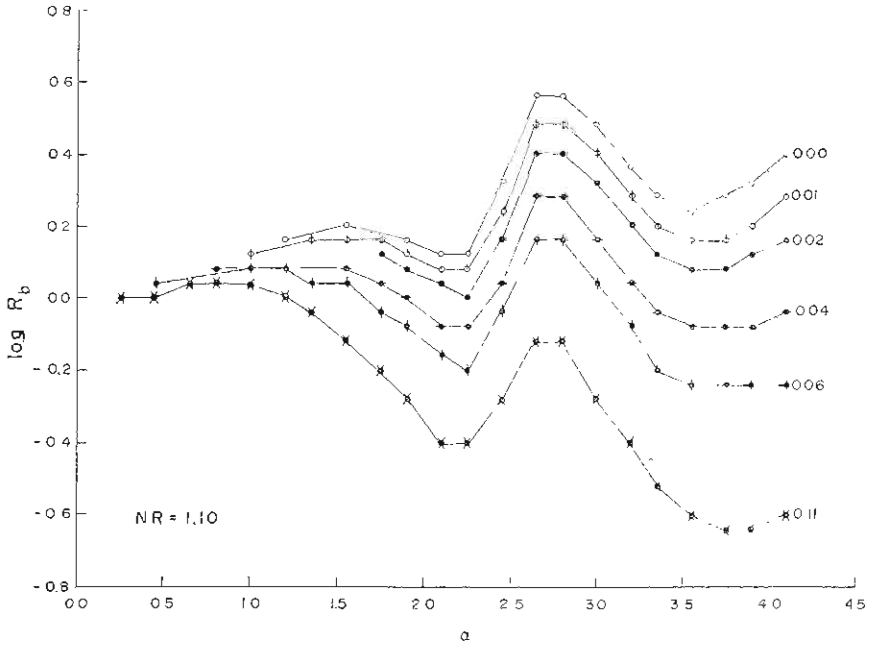


Figure 7 - Same as Figure 3 for  $R_b$ .

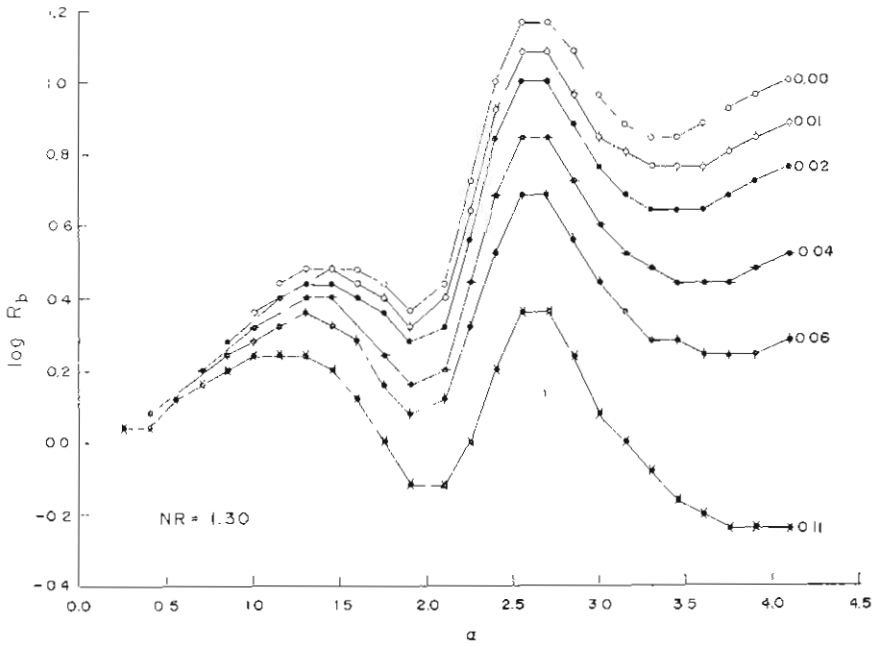


Figure 8 - Same as Figure 4 for  $R_b$ .

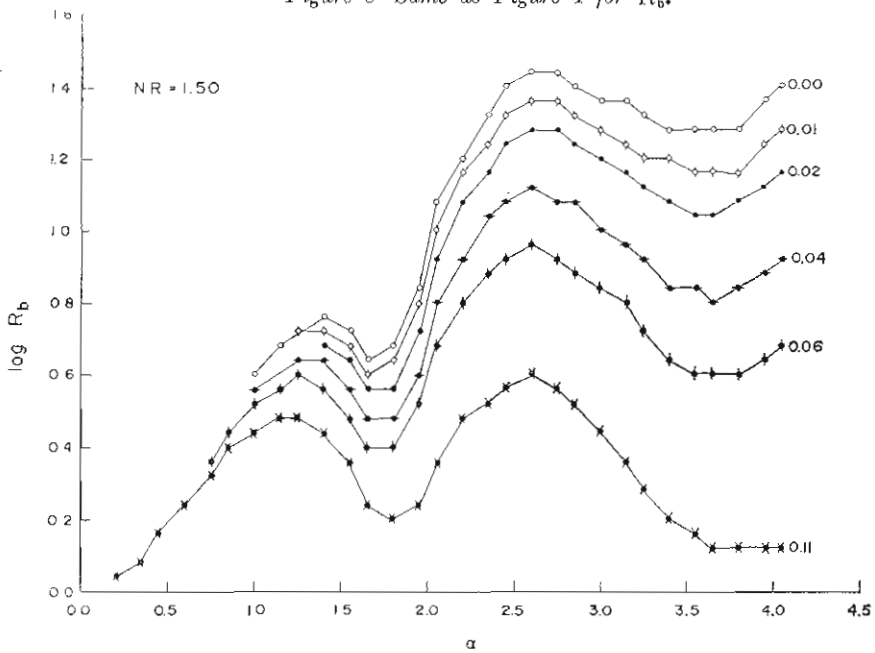


Figure 9 - Same as Figure 5 for  $R_b$ .

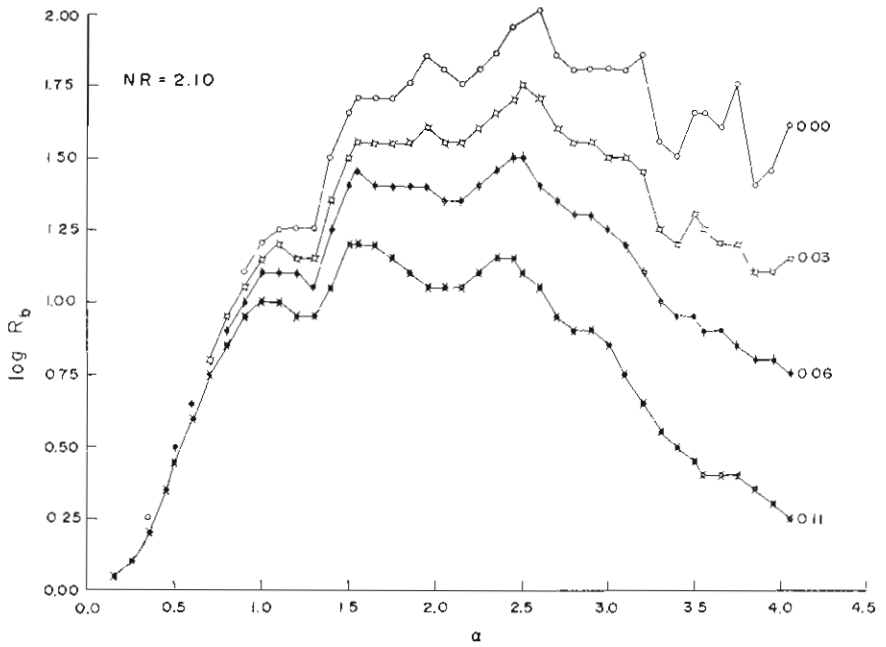


Figure 10 - Same as Figure 6 for  $R_b$ .



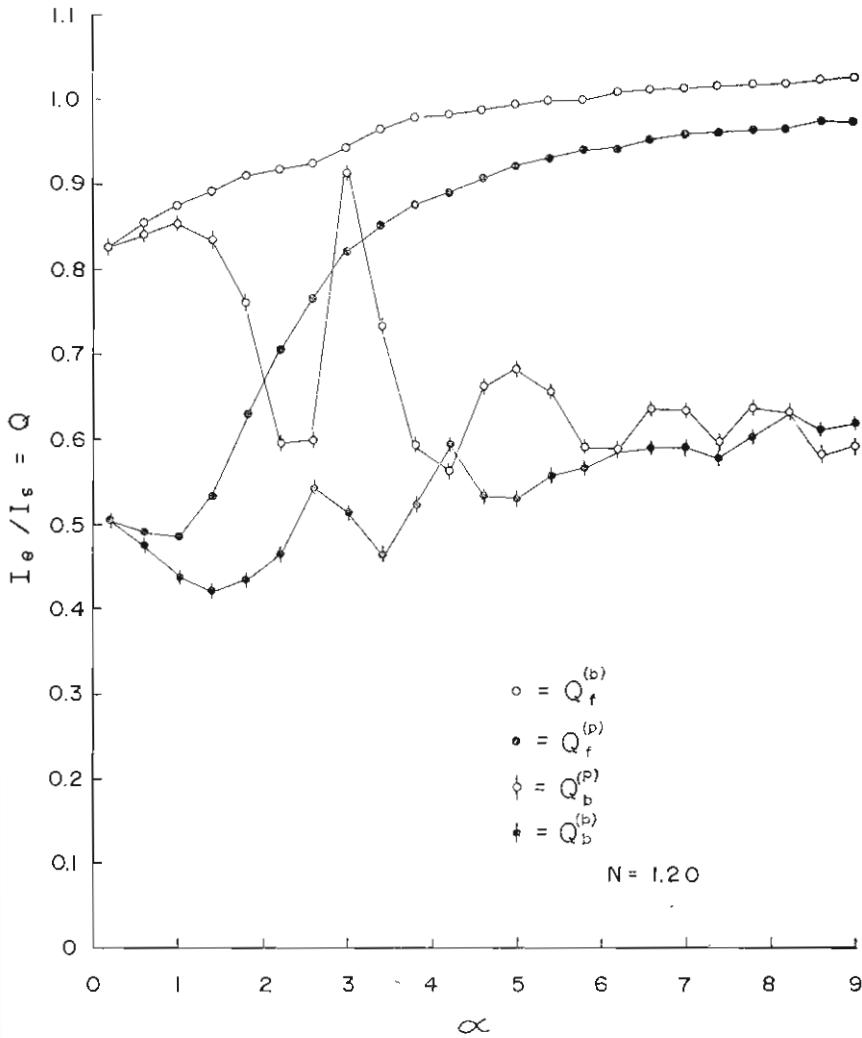


Figure 11 - The dependence on  $\alpha$  of the ratio  $Q = I_e / I_s$  = ratio of the electromagnetic and scalar cross - sections in the forward and backward hemispheres for particles and bubbles for  $N = 1.20$ .

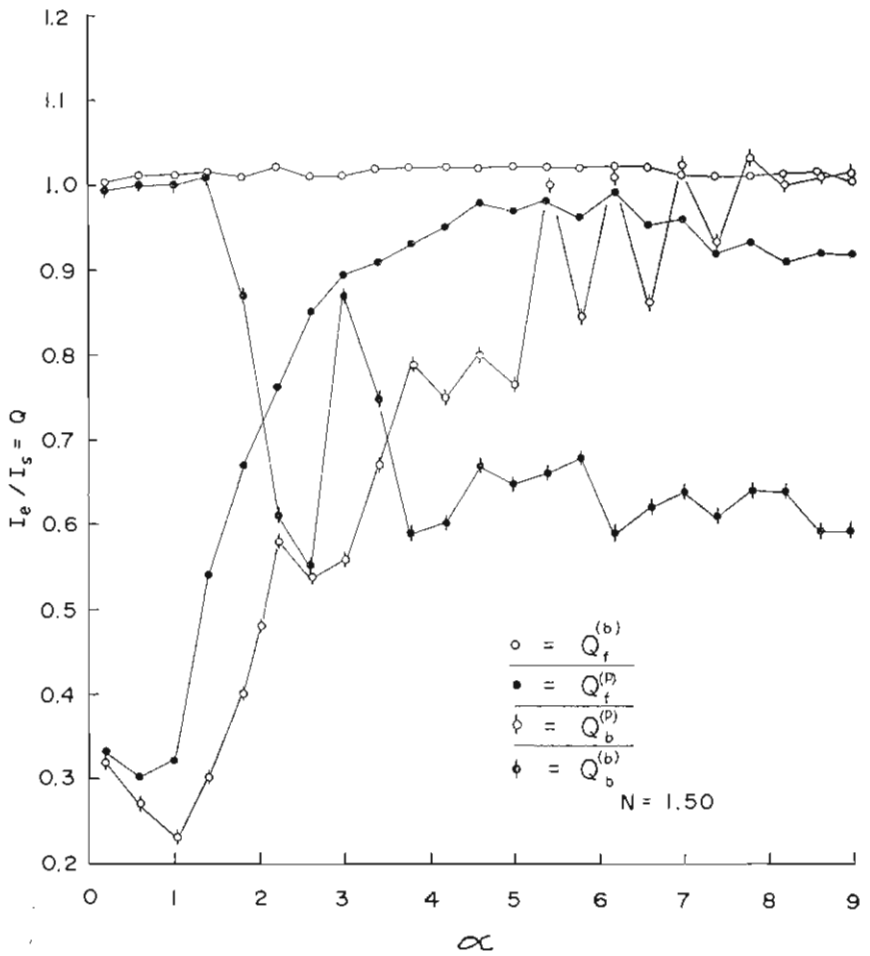


Figure 12 - Same as Figure 11 for  $N=1.50$ .

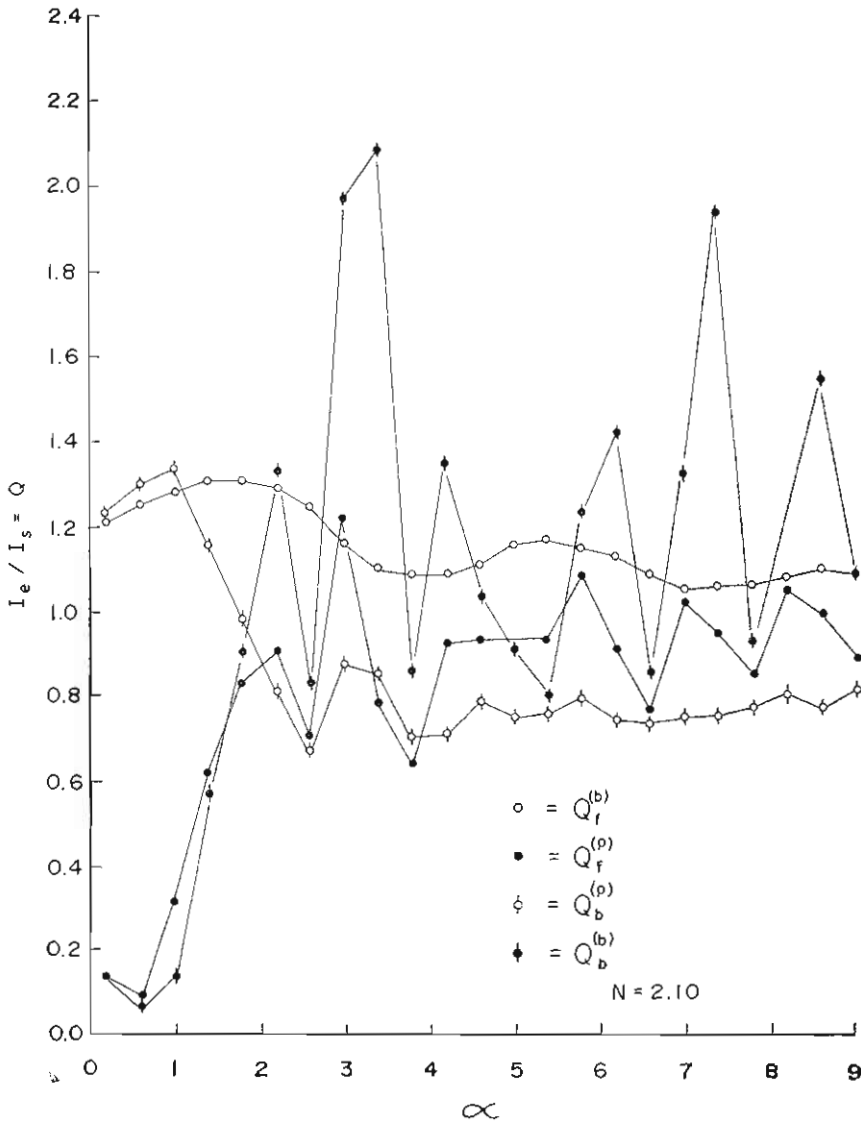


Figure 13 - Same as Figure 11 for  $N=2.10$ .

## REFERENCES

1. DAVE, J. V., IBM Scientific Center, 2760 Hanover St., Palo Alto, CA.
2. DENMAN, H. H., (1966) HELLER, W., and PANGONIS, W. J., «Angular Scattering Functions for Spheres», Wayne State University Press, Detroit.
3. PATITSAS, A. J., (1972) Can. J. Phys. 50, 3172.
4. PATITSAS, A. L., (1971) Can. J. Phys. 49, 1924.
5. ROSCH, S., (1968) Appl. Opt. 7, 233.
6. STONE, J. M., (1963) «Radiation and Optics» McGraw - Hill Book Co., Inc., New York.
7. STRATTON, J. A., (1941) «Electromagnetic Theory». McGraw - Hill Book Co., Inc., New York,

## ΠΕΡΙΛΗΨΗ

# ΣΥΓΚΡΙΣΗ ΤΩΝ ΔΙΑΤΟΜΩΝ ΣΚΕΔΑΣΕΩΣ ΣΦΑΙΡΙΚΩΝ ΣΩΜΑΤΙΩΝ ΚΑΙ ΦΥΣΑΛΛΙΔΩΝ

ύπό

Α. ΠΑΤΙΤΣΑ

Ἡ ἀπ' εὐθείας καὶ ἡ κατὰ τὴν ἀντίθετη κατεύθυνση διατομὴ σκεδάσεως ἐνὸς σφαιρικοῦ σωματίου μὲ ἀκτίνα  $a$  καὶ μιγαδικὸ δείκτη διαθλάσεως  $N_1$  ποὺ βρίσκεται σὲ ἓνα μέσο μὲ πραγματικὸ δείκτη διαθλάσεως  $N_2$  καὶ οἱ ἴδιες δραστηκῆς διατομῆς σφαιρικῆς φυσαλλίδας μὲ ἀκτίνα  $a$  καὶ πραγματικὸ δείκτη διαθλάσεως  $N_2$  ποὺ βρίσκεται σὲ ἑλαφρὸ ἀγώγιμο μέσο μὲ μιγαδικὸ δείκτη διαθλάσεως  $N_1$  ( $|N_1| > N_2$ ), προσδιορίζονται καὶ συγκρίνονται στὴ περιοχὴ τοῦ Rayleigh, ὅπου  $\alpha = 2\pi a/\lambda \leq 0.3$  καὶ ἐπίσης ὑπολογίζονται καὶ συγκρίνονται στὴν περιοχὴ τοῦ Mie,  $0.3 < \alpha \leq 22.0$ . Τὸ πραγματικὸ μέρος τοῦ δείκτη διαθλάσεως  $N = N_1/N_2$  παίρνει τὶς τιμῆς 1.1, 1.3, 1.5, 2.1, ἐνῶ τὸ φανταστικὸ μέρος τοῦ  $N$  μεταβάλλεται μὲ μικρὰ βήματα ἀπὸ 0.01 ἕως 0.11. Οἱ λόγοι τῶν διατομῶν σκεδάσεως τοῦ σωματίου καὶ αὐτῶν τῆς φυσαλλίδας παρουσιάζονται σὲ γραφικὴ μορφή. Ἡ βαθμωτὴ θεωρία χρησιμοποιεῖται ἐπίσης στὸν ὑπολογισμὸ τῆς διατομῆς σκεδάσεως σωματίων καὶ φυσαλλίδων καὶ τὰ ἀποτελέσματα συγκρίνονται σὲ γραφικὴ μορφή μὲ ἐκεῖνα ποὺ βασίζονται στὴ θεωρία τοῦ Mie.